

# Preparation of Size-Controlled TiO<sub>2</sub> Nanoparticles and Derivation of Optically Transparent Photocatalytic Films

Seung Yong Chae, Myun Kyu Park, Sang Kyung Lee, Taek Young Kim, Sang Kyu Kim,<sup>†</sup> and Wan In Lee\*

Department of Chemistry, Inha University, Incheon, 402-751 Korea

Received February 7, 2003. Revised Manuscript Received June 10, 2003

TiO<sub>2</sub> nanoparticles were prepared by hydrothermal reaction of titanium alkoxide stabilized in acidic ethanol/water solution. The sizes of particles have been controlled to the range of 7–25 nm by adjusting the concentration of Ti precursor and the composition of the solvent system. The TiO<sub>2</sub> samples synthesized under this acidic ethanol/water environment were mainly primary particles in anatase phase without secondary structure. The suspension of as-prepared 7-nm-sized TiO<sub>2</sub> nanoparticles demonstrates long-term stability, and has been applied successfully for the fabrication of ultra-transparent particulate TiO<sub>2</sub> films. The photocatalytic efficiency of TiO<sub>2</sub> films prepared from the 7-nm-sized nanoparticles was 1.6 times of that of films derived from Degussa P25 in decomposing gaseous 2-propanol.

## Introduction

With its unique characteristics in band position and surface structure, TiO<sub>2</sub> in thin film form has promising application as a photocatalyst for decomposing organic pollutants,<sup>1–6</sup> and as a self-cleaning and super-hydrophilic smart material.<sup>7–11</sup> For these commercial applications, the fabrication of optically transparent TiO<sub>2</sub> films at low temperature and in large area will be crucial issues, because those films are, in general, applied on the surface of soda-lime glass, paper, or plastic.

Recently, derivation of films by coating the suspension of nanoparticles has attracted special attention as a new technique for the fabrication of thin and thick films. This technique has several advantages over other film-deposition techniques, especially for TiO<sub>2</sub> films.<sup>12–14</sup> The

major advantage is that it provides for a low-temperature fabrication process, as each nanoparticle consisting of film is already in crystallized form. Ultimately, room-temperature deposition can be achieved if inorganic binders hardening at ambient condition are introduced to the suspension of nanoparticles. In addition, it is an economical process and large-area deposition can be achieved easily. On the other hand, the demerits of this method are poor adhesion of films onto the substrate, and lack of surface uniformity. The adhesion problem can be mitigated with the addition of inorganic binders, such as siloxane derivatives, to the TiO<sub>2</sub> suspension prior to coating. A more critical problem would be poor surface uniformity of the films. In the suspension, individual TiO<sub>2</sub> particles are heavily agglomerated to decrease the surface energy, and the agglomerated particles are hardly broken by physical suspending methods. For example, the average diameter of colloids for the aqueous suspension of Degussa P25 TiO<sub>2</sub> is approximately 300–500 nm, even though the average size of an individual particle is only 25 nm. Even though the issues on the inter-particle agglomeration in the suspension are solved completely, the ultimate limit of surface roughness for the derived film will correspond to the diameter of each nanoparticle. Therefore, to achieve high-quality films by coating the suspensions of nanoparticles, the size of an individual particle should be smaller than the desired roughness of the film, and the long-term stability of the suspension without agglomeration or precipitation is prerequisite.

The preparation of TiO<sub>2</sub> nanoparticles in solution phase would be one of the best synthetic routes, both for controlling the size of individual particles and for obtaining the stabilized colloidal suspensions. TiO<sub>2</sub> nanoparticles have been synthesized from the hydrolysis of TiCl<sub>4</sub>, titanium isopropoxide, or titanyl sulfate-based

\* To whom correspondence should be addressed. E-mail: wanin@inha.ac.kr.

<sup>†</sup> Present address: Department of Chemistry and School of Molecular Sciences, Korea Advanced Institute of Science and Technology (KAIST), Daejeon, 305-701, Korea.

- (1) Turchi, C. S.; Ollis, D. F. *J. Catal.* **1990**, *122*, 178.
- (2) Matthews, R. W. *J. Catal.* **1998**, *111*, 264.
- (3) Nozik, A. J. *Annu. Rev. Phys. Chem.* **1978**, *29*, 189.
- (4) Hoffmann, M. R.; Martin, S. T.; Choi, W.; Bahnemann, D. W. *Chem. Rev.* **1995**, *95*, 69.
- (5) Pelizzetti, E. *Sol. Energy Mater. Sol. Cells* **1995**, *38*, 453.
- (6) Taborda, A. V.; Brusa, M. A.; Grela, M. A. *Appl. Catal. A: General* **2001**, *208*, 419.
- (7) Miyauchi, M.; Nakajima, A.; Watanabe, T.; Hashimoto, K. *Chem. Mater.* **2002**, *14*, 2812.
- (8) Yamazaki-Nishida, S.; Cervera-March, S.; Nagno, K. J.; Anderson, M. A.; Hori, K. *J. Phys. Chem.* **1995**, *99*, 15814.
- (9) Vinodgopal, K.; Stafford, U.; Gray, K. A.; Kamat, P. V. *J. Phys. Chem.* **1994**, *98*, 6797.
- (10) Wang, R.; Hashimoto, K.; Fujishima, A.; Chikuni, M.; Kojima, E.; Kitamura, A.; Shimohigoshi, M.; Watanabe, T. *Nature* **1997**, *388*, 431.
- (11) Wang, R.; Hashimoto, K.; Fujishima, A.; Chikuni, M.; Kojima, E.; Kitamura, A.; Shimohigoshi, M.; Watanabe, T. *Adv. Mater.* **1998**, *10*, 135.
- (12) Gao, Y.-M.; Shen, H.-S.; Dwight, K.; Wold, A. *Mater. Res. Bull.* **1992**, *27*, 1023.
- (13) Negishi, N.; Takeuchi, K.; Ibuski, T.; Datye, A. K. *J. Mater. Sci. Lett.* **1999**, *18*, 515.

(14) Kamat, P. V. *Chemtech* **1995**, (June), 23.

precursors in acidic condition,<sup>15–22</sup> and from the reverse micelle methods in nonpolar solvent with surfactants.<sup>23–26</sup> So far considerable progress has been achieved in the synthesis of titania nanoparticles, but further studies still have to be exerted for the control of particle size, crystallization in the form of primary particle, and the inhibition of inter-particular aggregation. In this work, we stabilized titanium isopropoxide in acidic ethanol/water solution prior to hydrothermal reaction. The addition of ethanol may affect the size control of titania nanoparticles by stabilization of Ti precursor, whereas the hydrothermal condition induces a high crystallization.

Previously, we modified the surface of Degussa P25 TiO<sub>2</sub> with highly acidic metal oxides, such as WO<sub>3</sub> or MoO<sub>3</sub>.<sup>27,28</sup> The colloidal particles were less agglomerated, and their average colloid sizes in the aqueous suspension were decreased  $1/4$ – $1/5$ , compared with that of pure TiO<sub>2</sub>. As a result, the surface uniformity of derived films was notably improved. In the present work, we have synthesized 7-nm TiO<sub>2</sub> particles, which is less than  $1/3$  the size of Degussa P25. With applying this suspension, the uniformity of particulate TiO<sub>2</sub> films was further improved. The surface and optical properties of derived films were characterized, and their photocatalytic activity was also analyzed.

### Experimental Section

Titanium isopropoxide (97%, Aldrich Chemical Co.; 1.5–15 mmol) was added dropwise to 150 mL of mixed ethanol and water solution. The solution pH was adjusted to 0.7 by adding nitric acid. In this acidic ethanol/water environment, the Ti precursor remained in clear solution without precipitation. After several hours of stirring, the clear solution was transferred to a glass-lined hydrothermal bomb, and then reacted at 240 °C for 4 h. After hydrothermal reaction the crystallized TiO<sub>2</sub> nanoparticles were obtained as a colloidal suspension. They were mainly primary particles without secondary structures, and the particle sizes were controlled to 7–25 nm by adjusting reaction parameters. To obtain powdered TiO<sub>2</sub> samples the suspensions were vacuum-dried at room temperature.

To be used for the coating solution, the concentration of as-prepared TiO<sub>2</sub> suspensions was adjusted to 1.0 g of TiO<sub>2</sub> in 30 mL by evaporating the solvent with a rotary evaporator. Then the concentrated suspensions were further dispersed by an

ultrasonic horn operated at 300 W, 20 kHz. The prepared suspension was spin-coated on Pyrex glass (2.5 × 2.5 cm<sup>2</sup>) at 2000 rpm for 40 s, and baked at 150 °C for 5 min. To obtain the films in desired thickness, the spin-coating and baking cycles were repeated. An approximate thickness of 100 nm was obtained from each spin-coating and baking cycle. Finally, the prepared TiO<sub>2</sub> films were annealed at 300 °C for 2 h in an oxygen environment to remove residual organics.

The average diameters of agglomerated TiO<sub>2</sub> nanoparticles in suspended aqueous solution were determined by a particle size analyzer (Zeta Master, Malvern Co.). The surface area of TiO<sub>2</sub> nanoparticles was determined using a nitrogen adsorption apparatus (model Gemini 2327, Micromeretics Instrument Corp., Norcross, GA). X-ray powder diffraction patterns for the TiO<sub>2</sub> nanoparticles were obtained by using a Philips diffractometer (PW3020) with a monochromated high-intensity Cu K $\alpha$  radiation. For the observation of synthesized nanoparticles by TEM (Philips CM30 transmission electron microscope operated at 250 kV), 1 mg of TiO<sub>2</sub> particle was dispersed in 50 mL of methanol and a drop of suspension was then spread on a holey amorphous carbon film deposited on Ni grid (JEOL Ltd.). The plan-view images of TiO<sub>2</sub> films derived from nanoparticles were observed by a field emission scanning electron microscope (FESEM, Hitachi S-4500). The surface roughness of film was examined by an atomic force microscope (AFM, TopoMetrix ACCUREX). Optical transmissions for the TiO<sub>2</sub> particles and films were recorded by UV–visible spectrophotometer (Perkin-Elmer Lambda 40) in the wavelength range of 200–900 nm.

The TiO<sub>2</sub> films derived from several nanoparticles were tested as photocatalyst for the decomposition of 2-propanol in gas phase. The gas reactor system used for this photocatalytic reaction is described elsewhere.<sup>28</sup> The net volume of the gastight reactor was 200 mL, and a TiO<sub>2</sub> film was located in the center of the reactor. The whole area of TiO<sub>2</sub> film (2.5 × 2.5 cm<sup>2</sup>) was irradiated by a 300 W Xe lamp through the 2-in. diam. silica window on the reactor. After evacuation of the reactor, 1.6  $\mu$ L of 2-propanol and 3.2  $\mu$ L of water were added. In the reactor their partial pressures were 2 and 16 Torr, respectively. The total pressure of the reactor was then controlled to 700 Torr by addition of oxygen gas. Under these conditions, 2-propanol and H<sub>2</sub>O remained in vapor phase. The gas mixtures in the reactor were magnetically convected during the irradiation. After the irradiation of a certain period of time, 0.5 mL of gas sample in the reactor was automatically picked up and sent to a gas chromatograph (Young Lin M600D) by using an autosampling valve system (Valco Instruments Inc. A60). For the detection of CO<sub>2</sub>, a methanizer was installed between the GC column outlet and the FID detector.

### Results and Discussion

**Preparation and Characterization of TiO<sub>2</sub> Nanoparticles.** The TiO<sub>2</sub> nanoparticles synthesized at ethanol-rich condition (ethanol/water, 4:1, in volume) were mainly in anatase with impurity phase of brookite, as indicated in the XRD patterns of Figure 1(a). The crystallinity of TiO<sub>2</sub> particles was gradually increased with the elevation of reaction temperature up to 240 °C. With further increase of reaction temperature up to 300 °C, their crystallinity was not appreciably changed. However, when the reaction temperature went up beyond 260 °C the primary particles began to be aggregated to larger secondary particles. Thus, 240–260 °C is considered to be optimum reaction temperature range.

The sizes of nanoparticles were greatly dependent on the concentration of titanium isopropoxide and on the ratio between ethanol and water in the solvent system. Conversely, they were less dependent on the reaction temperature or reaction time. First of all, the volume

- (15) Cheng, H.; Ma, J.; Zhao, Z.; Qi, L. *Chem. Mater.* **1995**, *7*, 663.
- (16) Barbé, C.; Arendse, F.; Comte, P.; Jirousek, M.; Lenzmann, F.; Shklover, V.; Grätzel, M. *J. Am. Ceram. Soc.* **1997**, *80*, 3157.
- (17) Iwasaki, M.; Hara, M.; Ito, S. *J. Mater. Sci. Lett.* **1998**, *17*, 1769.
- (18) Lee, S.-H.; Kang, M.; Cho, S. M.; Han, G. Y.; Kim, B.-W.; Yoon K. J.; Chung, C.-H. *J. Photochem. Photobiol. A* **2001**, *146*, 121.
- (19) Keshmiri, M.; Troczynski, T. *J. Non-Crystal. Solids* **2002**, *311*, 89.
- (20) Martin, S. T.; Herrmann, H.; Choi, W.; Hoffmann, M. R. *J. Chem. Soc., Faraday Trans.* **1994**, *90*, 3315.
- (21) Anpo, M.; Aikawa, N.; Kubokawa, Y. *J. Chem. Soc., Chem. Commun.* **1984**, 644.
- (22) Anpo, M.; Yamashita, H. In *Surface Photochemistry*; Anpo, M., Ed.; John Wiley & Sons: Chichester, U.K., 1996; p 117.
- (23) Stathatos, E.; Tsiourvas, D.; Lianos, P. *Colloids Surf. A* **1999**, *149*, 49.
- (24) Moran, P. D.; Bartlett, J. R.; Bowmaker, G. A.; Woolfrey, J. L.; Cooney, R. P. *J. Sol-Gel Sci. Technol.* **1999**, *15*, 251.
- (25) Stathatos, E.; Lianos, P.; Del Monte, F.; Levy, D.; Tsiourvas, D. *Langmuir* **1997**, *13*, 4295.
- (26) Trentler, T. J.; Denler, T. E.; Bertone, J. F.; Agrawal, A.; Colvin, V. L. *J. Am. Chem. Soc.* **1999**, *121*, 1613.
- (27) Song, K. Y.; Park, M. K.; Kwon, Y. T.; Lee, H. W.; Chung W. J.; Lee, W. I. *Chem. Mater.* **2001**, *13*, 2349.
- (28) Kwon, Y. T.; Song, K. Y.; Lee, W. I.; Choi, G. J.; Do, Y. R. *J. Catal.* **2000**, *191*, 192.

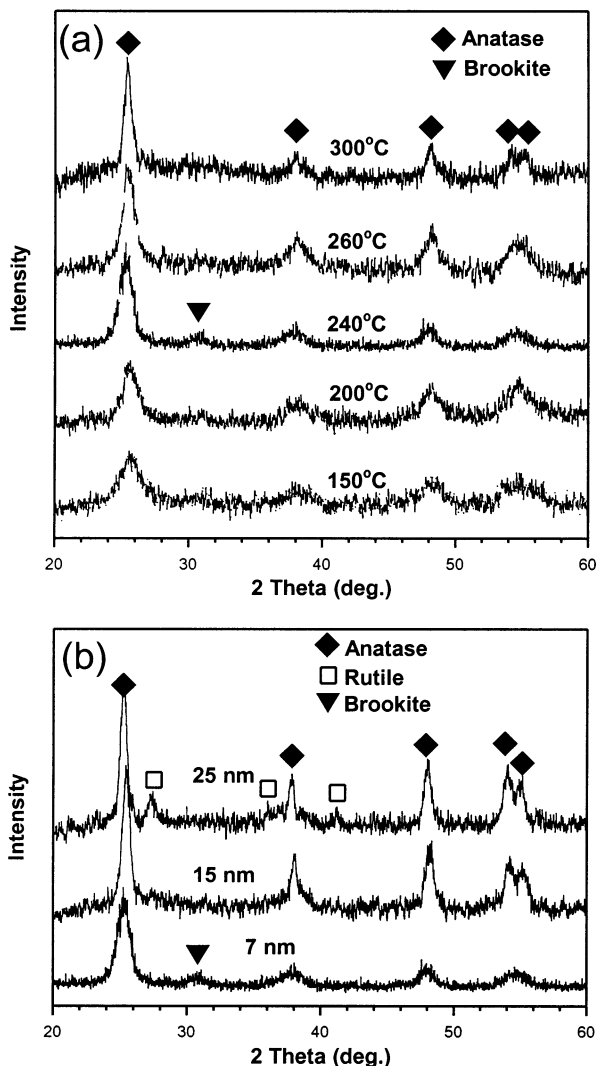


**Figure 1.** XRD patterns of  $\text{TiO}_2$  particles prepared by hydrothermal reaction at several temperatures (a) (the concentration of titanium isopropoxide was 0.10 M, and 4:1 ethanol/water was used as the solvent system), and those of  $\text{TiO}_2$  particles of different sizes synthesized at 240 °C for 4 h (b).

ratio between ethanol to water was varied from 0 to  $\infty$ , while the condition for hydrothermal reaction was fixed to 240 °C for 4 h, and the concentration of titanium isopropoxide was adjusted to 0.10 M. Figure 2(a) indicates that the size of  $\text{TiO}_2$  nanoparticle is gradually decreased with the increase of ethanol-to-water ratio. In pure water, the size of obtained  $\text{TiO}_2$  particle was 21–23 nm, but in the ethanol-rich condition, such as in 4:1–8:1 ethanol/water ratio, the particle size went down to 7 nm. If the ethanol-to-water ratio was higher than 8, however, the  $\text{TiO}_2$  particles were poorly crystallized, and were aggregated with insufficient hydrolysis. In ethanol/water mixed solution the hydrolyzed titanium isopropoxide could be stabilized without precipitation by adjusting the solution pH to about 0.7 with nitric acid. At lower pH than 0.7 the rutile phase was incorporated to the anatase-based nanoparticles. At higher pH the stabilization of titanium precursor was not successful, and the solution changed to slightly milky.

The effect of titanium isopropoxide concentration was described in Figure 2b. The condition for hydrothermal

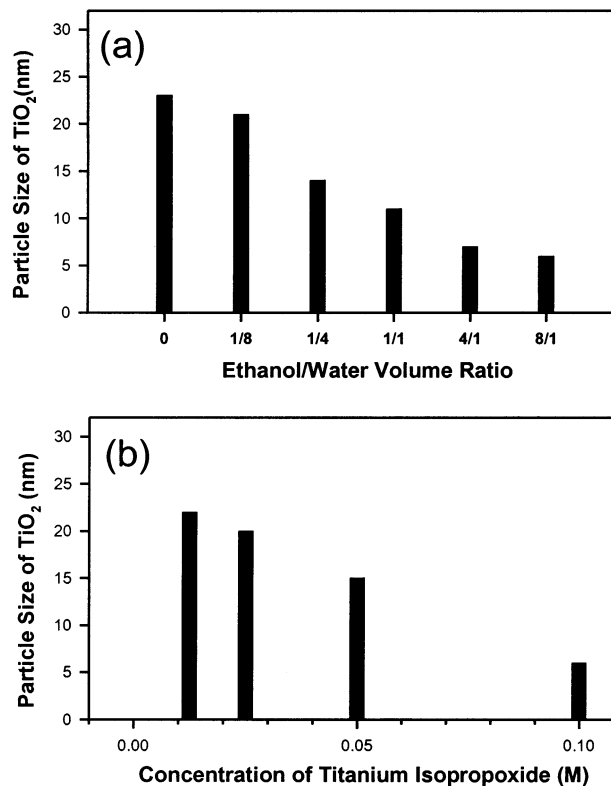


**Figure 2.** Variation of  $\text{TiO}_2$  particle size with reaction parameters: dependence on ethanol/water ratio (a) (the concentration of titanium isopropoxide was kept to 0.10 M), and dependence on titanium isopropoxide concentration (b) (the ethanol/water ratio was 4:1). Particles were synthesized at 240 °C for 4 h in a hydrothermal bomb.

reaction was fixed to 240 °C for 4 h, and the volume ratio of ethanol to water was kept to 4:1. The sizes of  $\text{TiO}_2$  nanoparticles were gradually decreased with increasing the concentration of titanium isopropoxide from 0.010 to 0.10 M. It is assumed that the greater number of  $\text{TiO}_2$  nuclei is evolved under higher concentration of titanium isopropoxide during the hydrothermal reaction at 240 °C. Thus, the grain growth for each nucleated  $\text{TiO}_2$  is suppressed with mutual competition, and this leads to the formation of small-sized  $\text{TiO}_2$  nanoparticles. At higher concentration over 0.10 M, however,  $\text{TiO}_2$  particles were clogged together.

As shown in the TEM images of Figure 3, the sizes of  $\text{TiO}_2$  nanoparticles can be controlled from 7 to 25 nm by varying the composition of solvent system and the concentration of titanium isopropoxide. Typically, the 7-nm-sized  $\text{TiO}_2$  nanoparticle was formed with 0.10 M titanium isopropoxide in 4:1 ethanol/water solution, whereas the 25-nm-sized particle was obtained with 0.02 M titanium isopropoxide in 1:8 ethanol/water. In addition,  $\text{TiO}_2$  nanoparticles of 15 nm could be obtained by using 0.04 M titanium isopropoxide in 1:2 ethanol/water. The 7-nm particles were also analyzed by high-resolution TEM, as shown in Figure 3(d). The uniform lattice fringes observed over an entire  $\text{TiO}_2$  particle indicate that the individual particle consists of a single grain.

XRD patterns for the 7-, 15-, and 25-nm  $\text{TiO}_2$  particles are shown in Figure 1(b). Particles of 7 and 15 nm are mostly in anatase phase, but the 25-nm particle contains rutile impurities. Cheng et al. have reported that in the



**Table 1. Characterization Results for the Several TiO<sub>2</sub> Nanoparticles**

	7 nm	15 nm	25 nm	P25
crystallite size (nm)	6.4	14	20	20
surface area (m <sup>2</sup> /g)	190	124	75	60
calculated surface area (m <sup>2</sup> /g)	220	102	60	60
volume average of colloid size in suspension (nm)	40	195	290	410
crystallographic phase <sup>a</sup>	A/B = 92:8	A	A/R = 80:20	A/R = 70:30

<sup>a</sup> A, anatase; B, brookite; R, rutile phase.

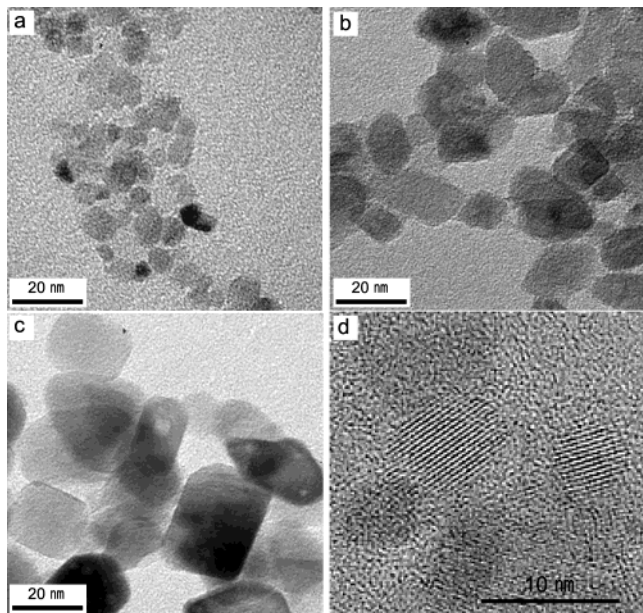


**Figure 3.** TEM images of 7-nm-sized TiO<sub>2</sub> nanoparticles prepared from 0.10 M titanium isopropoxide in 4:1 ethanol/water (a), 15-nm particles prepared from 0.04 M titanium isopropoxide in 1:2 ethanol/water (b), 25-nm particles prepared from 0.02 M titanium isopropoxide in 1:8 ethanol/water (c), and a high-resolution TEM image for a 7-nm particle (d).

synthesis of TiO<sub>2</sub> particles by hydrothermal reaction in aqueous solution the rutile phase begins to be incorporated at pH 1.0, and its amount increases with further decrease of pH.<sup>16</sup> Thus, our observation for the rutile impurity in the 25-nm-sized TiO<sub>2</sub> particles prepared under water-rich condition (ethanol/water, 1:8) at pH 0.7 is substantially consistent with Cheng's report. On the other hand, the 7-nm-sized particles synthesized in ethanol-rich condition (ethanol/water, 4:1) at the same pH did not contain any rutile phase. This may be explained by particle size effect.

The crystallite sizes of TiO<sub>2</sub> particles were calculated from each 101 peak shown in Figure 1(b). As illustrated in Table 1, the crystallite sizes determined from Scherrer equation were 6.4, 14, and 20 nm, respectively. For the 7- and 15-nm particles, the calculated value is coincident with the size of particles obtained from TEM images. This provides the evidence that the prepared TiO<sub>2</sub> nanoparticles are composed of single grains, and that they are mostly primary particles without secondary structure.

The surface areas for the individual particles measured by BET method are also given in Table 1. The measured surface area of the 7-nm particle was 190 m<sup>2</sup>/g, whereas that of Degussa P25 in 25 nm size was 60 m<sup>2</sup>/g. Approximately, the surface area for each particle was inversely proportional to the particle size. The surface areas for the prepared nanoparticles have been

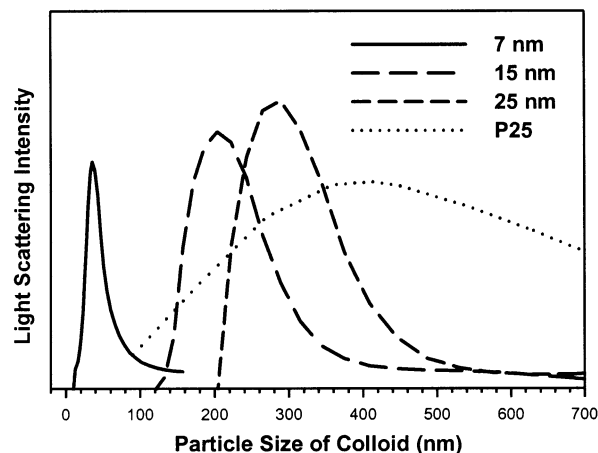
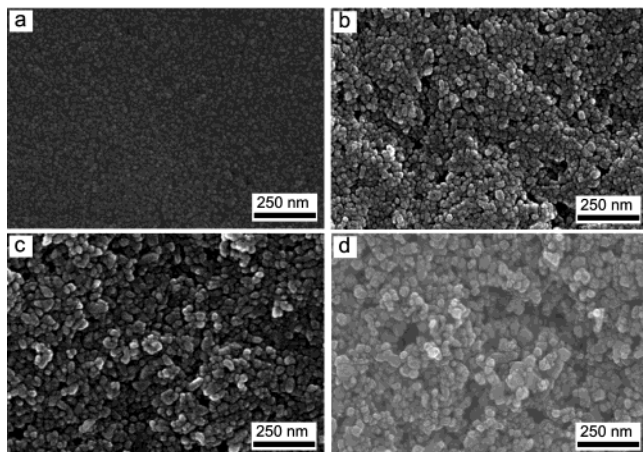


**Figure 4.** Particle size distributions in volume for several as-prepared TiO<sub>2</sub> suspensions.

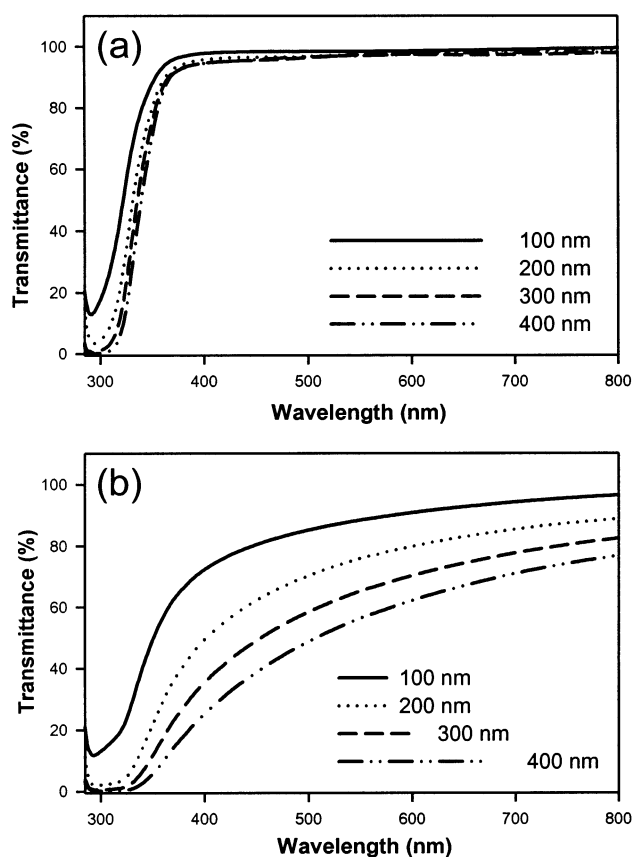
calculated by assuming that each particle is a spherical shape without pores or internal surface. As indicated in Table 1, the measured surface areas for the 7-, 15-, and 25-nm nanoparticles were similar to the calculated values. This suggests that the prepared TiO<sub>2</sub> nanoparticles are close to spherical shape, and they are dense in structure without micropores or internal surface.

The as-prepared TiO<sub>2</sub> nanoparticles of 7 nm were ultra-stably suspended in solution (1.2 g of TiO<sub>2</sub> in 150 mL of ethanol/water mixture at pH 4.5). The sizes of agglomerated colloids in the suspensions were estimated with a particle size analyzer. The particle sizes in volume average are described in Figure 4. In the Degussa P25 colloidal suspension, the particle size in volume average was 410 nm, while that of 7-, 15-, and 25-nm particles was 40, 195, and 290 nm, respectively. The size of colloidal particle for the suspension of 7-nm-sized TiO<sub>2</sub> was significantly smaller than the others. On average, less than 200 individual TiO<sub>2</sub> particles are agglomerated to form a colloid in this suspension. The Zeta potential for the 7-nm TiO<sub>2</sub> particles suspended in aqueous solution of pH 7 was -0.009 V, while that of Degussa P25 was +0.013 V. The isoelectric point for this TiO<sub>2</sub> was around pH 8–9.

**Characterization of TiO<sub>2</sub> Particulate Films.** The TiO<sub>2</sub> nanoparticles suspended in ethanol/water were used for the deposition of particulate TiO<sub>2</sub> films. The concentration of TiO<sub>2</sub> in suspension was adjusted to 1.0 g per 30 mL of solution. A spin coating method was applied for the preparation of TiO<sub>2</sub> film in Pyrex substrate. By a single coating with this suspension at 2000 rpm, the obtained TiO<sub>2</sub> layer was approximately 100 nm thick. FESEM images for the surface of films 300 nm thick, derived from several TiO<sub>2</sub> nanoparticles and Degussa P25 deposited on Pyrex glass, are shown in Figure 5. The plan-view images indicate that the size of a TiO<sub>2</sub> grain is coincident to its original particle size. The surface uniformities of TiO<sub>2</sub> films derived from

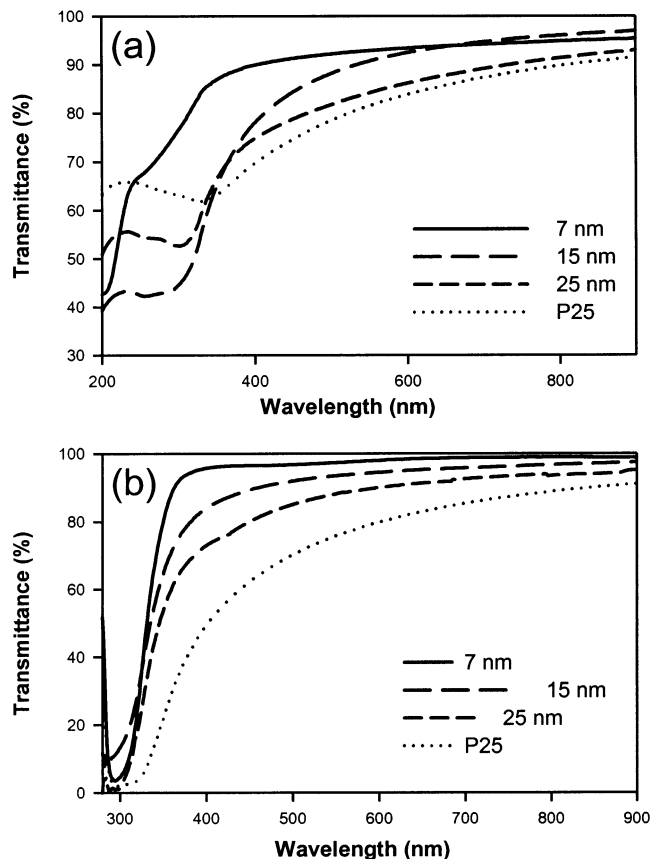


**Figure 5.** FESEM images for the surface of films derived from 7-nm (a), 15-nm (b), and 25-nm (c)  $\text{TiO}_2$  nanoparticles, and Degussa P25 (d). The thickness of each film was 200 nm.



**Figure 6.** Transmittance spectra for the  $\text{TiO}_2$  films derived from 7 nm-sized particles (a), and Degussa P25 (b). The thickness of films varied from 100 to 400 nm, and the transmittance spectra were obtained with a UV-visible spectrophotometer.

several nanoparticles were also observed by AFM. The average roughness of  $\text{TiO}_2$  films derived from 7-nm particles was 6 nm, and that of films from 15 and 25 nm were 14 and 23 nm, respectively, while that of films derived from P25 was 51 nm. As expected, the surface roughness was tantamount to the particle size of synthesized nanoparticles. Especially, the surface of particulate  $\text{TiO}_2$  films derived from 7-nm particles was so uniform that its surface uniformity was consistent with that of films derived from a typical sol-gel process or a sputtering method.



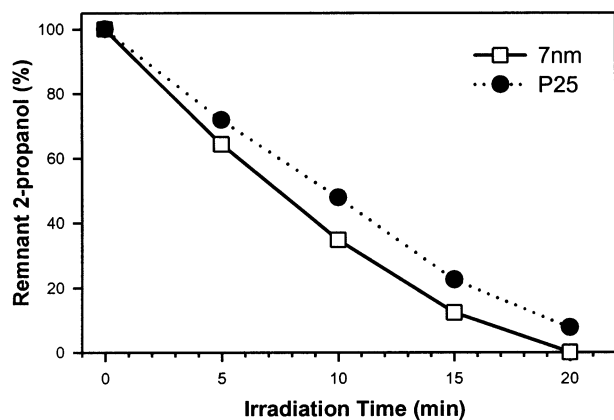
**Figure 7.** Transmittance spectra for the several suspensions of  $\text{TiO}_2$  nanoparticles (a), and the several  $\text{TiO}_2$  films derived from nanoparticles (b).  $\text{TiO}_2$  particles of 7, 15, and 25 nm, and P25 were used for these analyses. The concentration of suspensions was 1 mg of  $\text{TiO}_2$  in 100 mL of water, and the thickness of each film was 200 nm.

Figure 6(a) shows the transparency of particulate  $\text{TiO}_2$  films derived from 7-nm particles. Films in the thickness range of 100–400 nm looked optically clear, and demonstrated 98% of transmittance in the spectral range of 400–800 nm. Moreover, the transmittance was invariant with the increase of thickness, which was contrasted to the low transmittance of the films derived from Degussa P25, as shown in Figure 6(b).

To estimate band gap shift according to the size of  $\text{TiO}_2$  nanoparticles, 1.0 mg of each  $\text{TiO}_2$  sample was suspended in 100 mL of aqueous solution, and the absorption edges were measured by UV-visible spectrophotometer. As shown in the transmittance spectra of Figure 7(a), the absorption edges for the suspensions of 15- and 25-nm  $\text{TiO}_2$  and P25 were not appreciably different, but that of 7-nm  $\text{TiO}_2$  was considerably blue-shifted. This is indicative of a quantum size effect for the 7-nm  $\text{TiO}_2$ . The same experiment was performed for the particulate films derived from the  $\text{TiO}_2$  nanoparticles in different sizes. Differently from that of suspensions, however, the absorption edge of film samples was not shifted regardless of particle size, as indicated in Figure 7(b).

#### Photocatalytic Activity of $\text{TiO}_2$ Particulate Films.

The particulate  $\text{TiO}_2$  films prepared from 7-nm  $\text{TiO}_2$  nanoparticles were tested as a photocatalyst, and compared with that of  $\text{TiO}_2$  films derived from Degussa P25. Both particulate films were 300 nm thick. Gaseous 2-propanol was utilized as a model compound for the



**Figure 8.** Decomposition percentage of 2-propanol by the photocatalytic reaction with particulate TiO<sub>2</sub> films. In every 5 min of irradiation with a 300 W Xe lamp, the remaining percentage of 2-propanol was determined. The gas composition in the reactor was 2-propanol, 2.0 Torr; H<sub>2</sub>O, 16 Torr; and O<sub>2</sub>, 682 Torr.

evaluation of photocatalytic activity. It has been known that 2-propanol is primarily decomposed to acetone, and then finally decomposed to CO<sub>2</sub>.<sup>29</sup> Thus, the photocatalytic activity was estimated two ways. First of all, the decomposition of 2-propanol to acetone was monitored. Figure 8 describes the decomposition rates of 2-propanol with the films from 7-nm-sized TiO<sub>2</sub> and P25. The photocatalytic films derived from 7-nm-sized TiO<sub>2</sub> show appreciably faster decomposition than those from P25. Second, the amount of CO<sub>2</sub> evolved was evaluated. Figure 9 describes the amount of CO<sub>2</sub> evolved as a function of irradiation time. It was found that the CO<sub>2</sub> evolved in 20 min of irradiation with the films from 7-nm-sized TiO<sub>2</sub> was 1.6 times that evolved from P25. On the other hand, the photocatalytic films derived from 15- and 30-nm TiO<sub>2</sub> show lower photocatalytic efficiencies than those from P25. We believe that the particle size of TiO<sub>2</sub> affects the photocatalytic activity of particulate titania films. A detailed investigation for the particle size effect in determining photocatalytic activity is now in progress.

(29) Ohko, Y.; Hashimoto, K.; Fujishima, A. *J. Phys. Chem. A* **1997**, *101*, 8057.

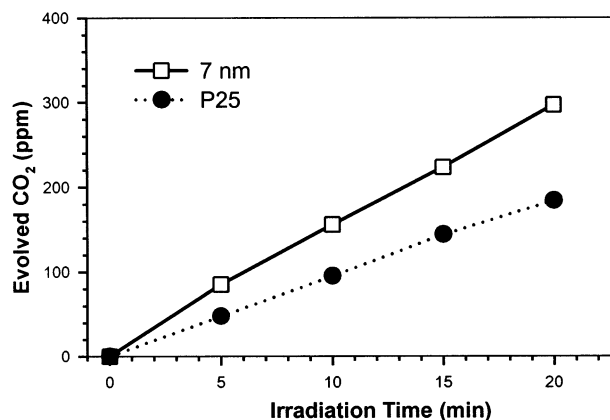


**Figure 9.** Photocatalytic oxidation rate of 2-propanol to CO<sub>2</sub> with particulate TiO<sub>2</sub> films. In every 5 min of irradiation with a 300-W Xe lamp, the concentration of CO<sub>2</sub> evolved was determined. The gas composition in the reactor was 2-propanol, 2.0 Torr; H<sub>2</sub>O, 16 Torr; and O<sub>2</sub>, 682 Torr.

### Conclusions

TiO<sub>2</sub> nanoparticles can be controlled from 7 to 25 nm by adjusting the solvent system and concentration of titanium precursor. The 7-nm TiO<sub>2</sub> nanoparticles were formed with 0.10 M titanium isopropoxide in 4:1 ethanol/water solution, whereas 25-nm particles were obtained with 0.02 M titanium isopropoxide in 1:8 ethanol/water solution. We also prepared 15-nm particles, by using 0.04 M titanium isopropoxide in 1:2 ethanol/water. The average colloidal size for this suspension was only 40 nm, and a quantum size effect was clearly observed. The particulate TiO<sub>2</sub> films derived from 7-nm particles were optically transparent: for the films 200 nm-thick the transmittance was 98% and the surface roughness was only 6 nm. The films derived from 7-nm nanoparticles demonstrate 1.6 times the photocatalytic activity of Degussa P25 in decomposing gaseous 2-propanol.

**Acknowledgment.** We gratefully acknowledge the financial support of the Korean Science and Engineering Foundation (KOSEF 2000-1-12200-002-3), and of the Korean Ministry of Commerce, Industry and Energy (Grant 00015875).

CM030171D